Exact topological quantum order in $D=3$ and beyond: Branyons and brane-net condensates

H. Bombin and M. A. Martin-Delgado
Departamento de Física Teórica I, Universidad Complutense, 28040 Madrid, Spain
(Received 4 August 2006; revised manuscript received 19 October 2006; published 7 February 2007)

We construct an exactly solvable Hamiltonian acting on a three-dimensional lattice of spin-$\frac{1}{2}$ systems that exhibits topological quantum order. The ground state is a string net and a membrane-net condensate. Excitations appear in the form of quasiparticles and fluxes, as the boundaries of strings and membranes, respectively. The degeneracy of the ground state depends on the homology of the 3-manifold. We generalize the system to $D \geqslant 4$, where different topological phases may occur. The whole construction is based on certain special complexes that we call colexes.

DOI: 10.1103/PhysRevB.75.075103 PACS number(s): 11.15.−q, 71.10.−w

I. INTRODUCTION

Deviations from a standard theory in a certain field of physics have always attracted attention in the search for new physics. In condensed matter, the standard model is the Landau theory of quantum liquids (Fermi liquid) supplemented with the spontaneous symmetry-breaking (SBB) mechanism and the renormalization group scheme.[1–3] The concept of local order parameter plays a central role in detecting quantum phases or orders within the Landau theory. Quite on the contrary, topological orders cannot be described by means of local order parameters or long-range interactions. Instead, a new set of quantum numbers is needed for this new type of phase, such as ground-state degeneracy, quasiparticle braiding statistics, edge states,[4–6] topological entropy,[7,8] etc.

A consequence of the SBB is the existence of a ground-state degeneracy. However, in a topological order, there exists a ground-state degeneracy with no breaking of any symmetry. This degeneracy has a topological origin. Thus, topological orders deviate significantly from more standard orders covered within the Landau symmetry-breaking theory. The existence of topological orders seems to indicate that nature is much richer than what the standard theory has predicted so far.

Emblematic examples of topological orders are fractional quantum Hall (FQH) liquids. FQH systems contain many different phases at $T=0$ which have the same symmetry. Thus those phases cannot be distinguished by symmetries and Landau's SBB does not apply.[4,9–11] Therefore we need to resort to other types of quantum numbers to characterize FQH liquids. For example, the ground-state degeneracy d_g depends on the genus g of the $D=2$ surface where the electron system is quantized; that is, $d_g=m^g$ with the filling factor being $\nu=\frac{1}{m}$.

There are several other examples of topological orders such as short-range resonating valence bond models,[12–15] quantum spin liquids,[5,16–23] etc. Due to this topological order, these states exhibit remarkable entanglement properties.[24,25] Besides these physical realizations, there have been other proposals for implementing topological orders with optical lattices,[26–28] with spin interactions in honeycomb lattices.[29] In this paper, we shall be concerned with topological models constructed with spins $S=\frac{1}{2}$ located at the sites of certain lattices with a coordination number, or valence, depending on the dimension D of the space and the color properties, which will be explained in Sec. II.

From the point of view of quantum information,[30] a topological order is a different type of entanglement: it exhibits nonlocal quantum correlations in quantum states. A topological phase transition is a change between quantum states with different topological orders. In dimensions $D \geqslant 4$, we construct exact examples of quantum lattice Hamiltonians exhibiting topological phase transitions in Sec. IV A. Here, we find an example of topology-changing transition as certain coupling constant is varied in $D=4$. This is rather remarkable since the most usual situation is to have an isolated topological point or phase surrounded by nontopological phases.[24,25]

In two dimensions, a large class of "doubled" topological phases has been described and classified mathematically using the theory of tensor categories.[47,48] The physical mechanism underlying this large class of topological orders is called string-net condensation. This mechanism is equivalent to particle condensation in the emergence of ordered phases in the Landau theory. A string net is a network of strings, and it is a concept more general than a collection of strings, either closed or open. In a string net, we may have a situation in which a set of strings meet at a branching point or node, something that is missing in ordinary strings which have two ends at most (see Fig. 14). More specifically, the ground state of these theories is described by superpositions of states representing string nets. The physical reason for this is the fact that local energy constraints can cause the local microscopic degrees of freedom present in the Hamiltonian to organize into effective extended objects such as string nets.

A different field of applications for topological orders has emerged with the theory of quantum information and computation.[31–34] Quantum computation, in a nutshell, is the art of mastering quantum phases to encode and process information. However, phases of quantum states are very fragile and decohere. A natural way to protect them from decoherence is to use topologically ordered quantum states which have a nonlocal kind of entanglement. The nonlocality means that the quantum entanglement is distributed among many different particles in such a way that it cannot be destroyed by local perturbations. This reduces decoherence significantly. Moreover, the quantum information encoded in the topological states can be manipulated by moving quasiparticle excitations around one another producing braiding effects that translate into universal quantum gates.[31,35–39]

Nevertheless, there are also alternative schemes to do lots of quantum information tasks by using only the entanglement properties of the ground state.[40–42]

The situation for topological orders in $D=3$ is less understood. This is due in part to the very intricate mathematical structure of topology in three dimensions. While the classification of all different topologies is well established in two dimensions, in $D=3$ the classification is much more difficult, and only recently does it appear to be settled with the proof of Thurston's geometrization conjecture,[43] a result that includes the Poincaré conjecture as a particular case.[44–46] Topological orders have been investigated in three dimensions with models that exhibit string-net condensation[47] using trivalent lattices that extend the case of trivalent lattices in two dimensions. However, a problem arises when one wishes to have an exactly solvable Hamiltonian describing this topological phase since this type of magnetic flux operators does not commute in three dimensions anymore. A solution to this problem can be found by imposing additional constraints to the mechanism found in $D=2$, but this somehow obscures the geometrical picture of the resulting exactly solvable model. Alternatively, it is possible to use a three-dimensional (3D) generalization of Kitaev's toric code to provide examples with a topological order based both on string condensation and on membrane condensation.[49] In the theory of topological quantum error correcting codes, there are also studies of toric codes in dimensions higher than $D=2$.[33,50,51]

In this paper, we introduce a solvable model in $D=3$ that exhibits a topological order. Here, we construct models in which local operators of several kinds commute among each other. This is achieved by requiring certain geometrical properties of the lattices, for which the models are defined. As a result, we can study the whole spectrum of the models and, in particular, their quantum topological properties. The ground state can be described as a string-net condensate or, alternatively, as a membrane-net condensate. A membrane-net condensate is a generalization of a collection of membranes, much like a string-net-condensate is a generalization of the notion of strings. Thus, in a membrane-net, membranes can meet at branching lines instead of at points. Excitations come in two classes: there are quasiparticles that appear as the end points of strings or certain type of fluxes that appear as the boundaries of membranes. These fluxes are extended objects. Interestingly enough, when a quasiparticle winds around a closed flux, the system picks up a nontrivial Abelian phase (see Fig. 17), very similar to when one anyon[52,53] winds around another anyon, acquiring an Abelian factor in the wave function of the system. We coin the name branyons to refer to this quasiparticles that are anyons with an extended structure. In fact, in our models they appear as Abelian branyons.

Our constructions can be nicely generalized to higher dimensions, where different classes of topological orders are possible. We can compute exactly the ground-state degeneracies in terms of the Betti numbers of the manifolds where the lattice models are defined. This allows us to discriminate between manifolds with different homological properties using quantum Hamiltonians. The generalized membranes are called branes, and we also find a brane-net mechanism.

We call the lattices that we introduce in this paper colexes. The motivation for their introduction is that they produce quantum Hamiltonians with a richer topology than others previously considered. For instance, in $D=2$ (see Ref. 40) we have constructed trivalent lattices on tori of genus g for which the ground-state degeneracy is 2^k, where k is given by $k=4-2\chi$, ($\chi=2-2g$ is the Euler characteristic), which is bigger by a factor of 2 than the degeneracy found in Kitaev's toric Hamiltonians. This factor of 2 is related to the appearance of two independent colors for the strings in the model.

In this paper, we have found a complete theory and properties of colexes of any dimension. In particular, we have found other instances of topological orders in $D=3$, where much little is known about the classification of topological orders as it is in $D=2$. The picture is even richer for $D\geqslant 4$ because different topological orders emerge from the same colex structure. We show how this is related to the fact that we can obtain several complexes from a single colex.

In order to summarize the main contributions that we present in this paper, we hereby advance a list of some of our most relevant results.

(i) We introduce a different class of exactly solvable models in $D=3$ and beyond based on a different type of lattices that we call D colexes (or colexes for short).

(ii) Our models present a different mechanism to generate topological orders in $D=3$ based on the concept of membrane-net condensation. Then, it is generalized to $D>3$ in terms of brane-net condensations.

(iii) In the excitation spectrum of these models, there are extended objects (not merely points) that exhibit nontrivial braiding properties. We call them branyons, which stands for brane anyons.

(iv) The ground-state degeneracy of our Hamiltonians has a topological origin, and it is different from those of other topological models. For instance, our models have higher degeneracy than Kitaev's toric codes.

(v) Colexes show a rich mathematical structure. The computation of topological invariants is reduced to a combinatorial problem. From a physical point of view, their structure gives rise to a remarkable property, namely, that the number of charges depends on the dimension of the space.

(vi) The topological structures exhibited by our models have natural applications in quantum information theory, where they can serve to construct topological quantum codes for error correction (see Ref. 40).

(vii) We have constructed families of Hamiltonians with topology-changing quantum phase transitions (see Sec. IV).

This paper is organized as follows. In Sec. II, we introduce the models defined in three-dimensional lattices placed on different manifolds. These lattices are constructed by means of color complexes that we call colexes of dimension 3, or 3-colexes. In Sec. III, the notion of colexes is generalized to arbitrary dimensions. In Sec. IV, we extend the topological quantum Hamiltonians beyond $D=3$ dimensions. In particular, we find instances of topology-changing phase transitions. Section V is devoted to conclusions. In a set of appendixes, we provide a full account of technical details pertaining to particular aspects of our models.

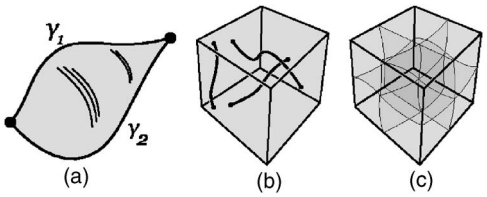

FIG. 1. In (a), the two curves are homologous because they form the boundary of a deformed disk. In (b) and (c), the 3-torus is represented as a cube in which opposite sides must be identified. In (b), a basis for 1-cycles is shown and in (c), a basis for 2-cycles.

II. THE MODEL IN 3-MANIFOLDS

A. Topological order and homology

The model that we are going to study belongs to the category of topologically ordered quantum systems. A system with topological quantum order is a gapped system that shows a dependency between the degeneracy of its ground state and the topology of the space where it exists. Certainly, such a dependency could manifest in many ways, typically as a function of certain topological invariants of the space.

In the case at hand, these topological invariants turn out to be the Betti numbers of the manifold. These in turn reflect the $\mathbf{Z}_2$ homology[42] of the manifold, and so we will now introduce several concepts and we will illustrate them using a well-known 3-manifold, the 3-torus.

Consider any 3-manifold $\mathcal{M}$. For a 1-cycle, we understand any closed nonoriented curve γ in it, or several such curves. In other words, it is a closed 1-manifold embedded in $\mathcal{M}$. Suppose that we can embed in $\mathcal{M}$ a 2-manifold in such a way that its boundary is γ. In that case, γ is called a 1-boundary and is said to be homologous to zero. More generally, consider two nonoriented curves γ_1 and γ_2 with common end points, as in Fig. 1(a). We can combine these two curves into a single 1-cycle, and then we say that they are homologous if the 1-cycle is a 1-boundary. In other words, $\gamma_1 \sim \gamma_2$ if and only if $\gamma_1+\gamma_2 \sim 0$. This kind of equivalence can also be applied to two 1-cycles, and thus two 1-cycles are homologous if and only if their combination is a 1-boundary. Then, the idea is that any 1-cycle can be constructed, up to homology equivalence, by a combination of certain basic 1-cycles. The number of 1-cycles needed to form such a basis is a topological invariant, the first Betti number h_1 of the manifold $\mathcal{M}$. For the 3-torus, $h_1=3$. A possible basis in this case is the one formed by the three 1-cycles that cross the torus in the three spatial directions, as in Fig. 1(b).

Similarly, we can think of 2-cycles as closed 2-manifolds embedded in $\mathcal{M}$. Then, when a 2-cycle is the boundary of some embedded 3-manifold, it is called a 2-boundary and is said to be homologous to zero. Two 2-manifolds with a common boundary can be sewn together to form a 2-cycle, and they are homologous if this 2-cycle is a 2-boundary. As in the case of 1-cycles, there exists a basis for 2-cycles up to homology. Again, these can be exemplified in the case of a 3-torus [see Fig. 1(c)]. The topological invariant that gives the cardinality of such a basis is the second Betti number h_2 and this equals h_1.

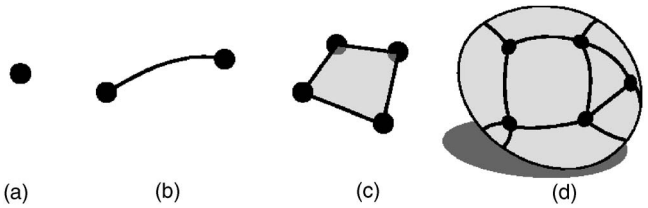

FIG. 2. (a) A vertex, (b) an edge, (c) a face, and (d) a polyhedral solid.

Throughout the text, we sometimes use a more suggestive language. Instead of curves, we talk about strings, closed or open with end points. Similarly, we refer to embedded 2-manifolds as membranes, either closed or with a boundary.

B. System and Hamiltonian

Usually, when we think of a lattice, say, a three-dimensional one, we first imagine or fix the space in which it exists. However, it is also natural to construct the space from the pieces that make up the lattice, say, its sites, links, and so on. Consider, for example, a football made up of hexagons and pentagons sewed together. In this case, the resulting topological space is a sphere made from several polyhedra that are attached, putting together vertices with vertices and sides with sides. Any closed 2-manifold can be constructed by sewing together polyhedra in this way. Such a construction is called a 2-complex, and its constituents are called general cells. Vertices are 0-cells, links are 1-cells, and the polyhedra or faces are 2-cells.

One can use these ideas for spaces of arbitrary dimension. In particular, we are now interested in three-dimensional spaces, which by analogy can be constructed by gluing together polyhedral solids. Let M be a closed connected manifold that has been constructed this way. Its polyhedral solids are balls whose boundary surface is a polyhedron, i.e., a sphere divided into faces, edges, and vertices (see Fig. 2). It is important that the gluing of polyhedral solids must be such that this structure is respected; that is, faces are glued to faces, edges to edges, and vertices to vertices. For brevity, we will call polyhedral solids simply cells. Thus, we have a 3-manifold divided into vertices V, edges E, faces F, and cells C. Such a structure in a 3-manifold is called a 3-complex.

In order to construct the topological quantum system that we propose, we consider a 3-complex such that (i) the neighborhood of every vertex is as the one in Fig. 3 and (ii) cells are four colored in such a way that adjacent cells have different colors. The colors we shall use are red, green, blue, and yellow (r,g,b,y). The main point of condition (i) is that the coordination of the lattice is 4, the minimum number to be able to construct interesting three-dimensional lattices. This first condition says more because it also states that six faces and four cells meet at each site in the most natural way. Thus, condition (i) states which is the local appearance of our lattice. As for condition (ii), its nature is global. Note that locally, at each site, it is immediately true. Moreover, we observe that at least four colors will be necessary to color any lattice satisfying (i) since at each site there are four dif-

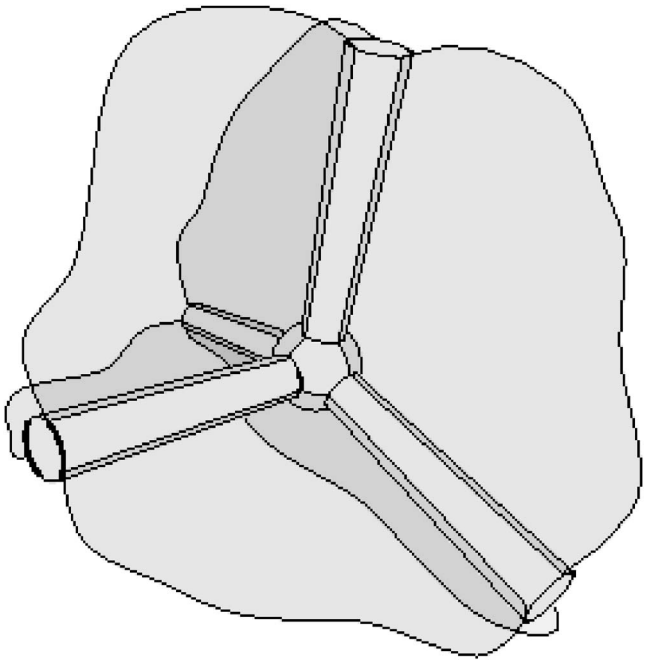

FIG. 3. The neighborhood of a vertex in a 3-colex. Four edges, six faces, and four cells meet at each vertex.

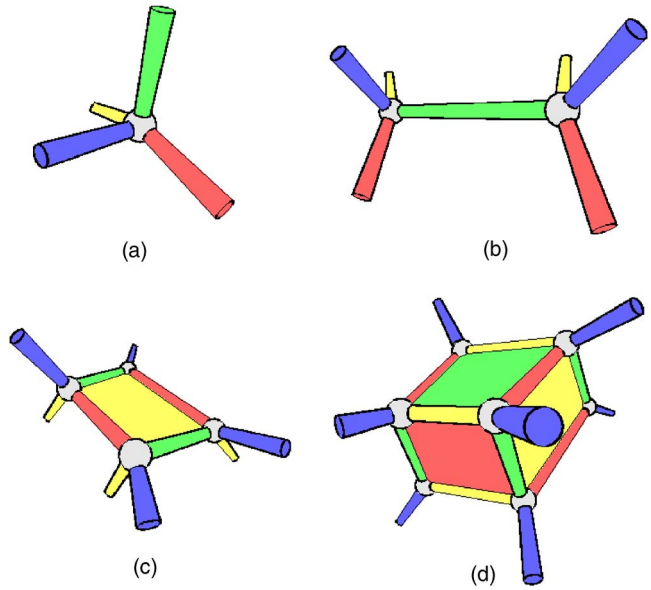

FIG. 4. (Color online) Neighborhoods in a 3-colex of (a) a vertex, (b) a g edge, (c) a by face, with the yellow side visible and the blue one hidden, and (d) a b cell. Faces are colored according to the color of the cell at their visible side.

ferent cells that meet. Condition (ii) is highly constraining, as we will show throughout this section. For example, the commutativity of the operators that sum up to give Hamiltonian (4) is contained in this condition.

We should stress that the name color does not imply that our lattices have to be colored with a new degree of freedom. The quantum degrees of freedom are always spin $\frac{1}{2}$ located at the sites of the colexes. In fact, we could have used another type of labeling in $D=3$ instead of using R,G,B,Y for $3+1$ colors. The important point here is the fact that color is introduced as a bookkeeping tool to keep track of the different sites, links, faces, and cells in the 3D lattice. We could have used another type of labeling, but we chose color because it is more appealing and facilitates the illustration of colexes in the figures.

From this point on, we will use assumptions (i) and (ii) to color edges and faces, and finally, we will see that the whole structure of the manifold is contained in the coloring of the edges.

With a glance at Fig. 3, we see that the four cells meeting at each vertex must have different colors. In the figure, we also see that each edge lies in three cells of different colors. Then each of the end points of the edge is in the corner of a cell of a fourth color, so that we can say that it connects two cells of the same color. We proceed to label edges with the color of the cells they connect [see Fig. 4(b)]. As a result, the four edges that meet at a vertex all have different colors [see Fig. 4(a)]. Also, the edges lying on a r cell are not r edges. However, much more is true. Consider r cell c and any vertex v in its boundary. The red edge that ends in v does not lie on cell c, so that the other three edges incident in v do. But then, any connected collection of g, b, and y edges corresponds exactly to the set of edges of some r-cells.

We label faces with two colors. If a face lies between a p cell and a q cell, we say that it is a pq face [see Fig. 4(c)]. Then consider, for example, a ry cell. Since neither r nor y edges can lie on its boundary, this must consist of a sequence of alternating b and g edges. Conversely, any such path is the boundary of some ry face. To check this, first note that exactly one such path traverses any given g edge e. But e must lie exactly on one ry face, the one that separates the r and the y cell it lies on.

As promised, we have shown that the entire structure of the manifold is contained in two combinatorial data: the graph and the colors of its edges. We call the resulting structure a 3-colex, for color complex in a 3-manifold. The simplest example of such a 3-colex with nontrivial homology is displayed in Fig. 5. It corresponds to the projective space P^3. In Appendix A, we will give a procedure to construct a colex of arbitrary dimension D, or D colex, starting with an arbitrary complex in a D manifold.

Although we shall be considering 3D manifolds with several different topologies in order to see the relationship between the ground-state degeneracy with the homology of the colex, we can also give now an example of a 3-colex in a more familiar closed manifold such as the 3D torus in condensed-matter systems. This is shown in Fig. 6. The virtue of this 3-colex is that it can fill the whole infinite space in case we want to take the thermodynamic limit along a family of lattices having the same topological properties. Thus far, we have only considered closed manifolds. Later, in Sec. II G, we shall also provide another example of a colex lattice with a boundary, so that our catalog of 3-colexes will be complete.

We now associate a physical system with the 3-colex. To this end, we place at each vertex (site) a spin-$\frac{1}{2}$ system. To each cell c, we attach the cell operator

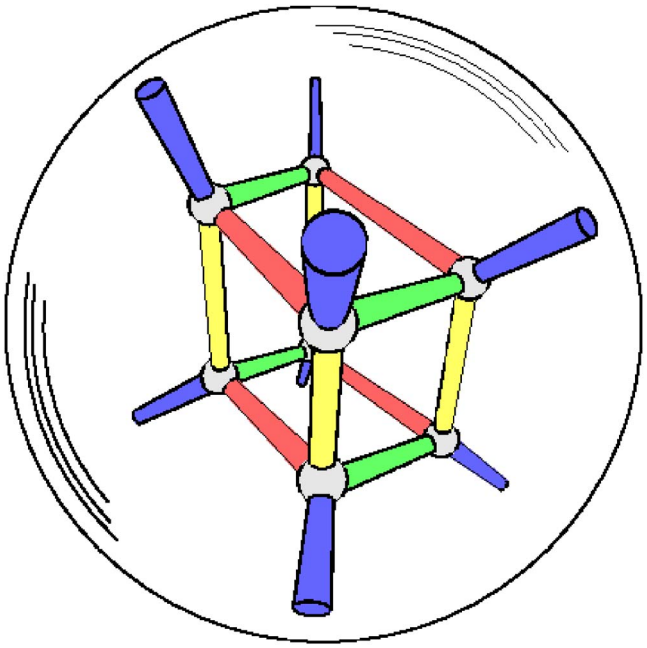

FIG. 5. (Color online) The projective space P^3 can be obtained starting with a solid sphere and identifying opposite points in its surface. Here, we use such a representation to show a 3-colex in P^3.

$$B_c^X := \bigotimes_{i \in I_c} X_i, \tag{1}$$

where X_i is the Pauli σ_1 matrix acting on site i and I_c is the set of sites lying on the cell. Similarly, to each face f we attach the face operator

$$B_f^Z := \bigotimes_{i \in I_f} Z_i, \tag{2}$$

where Z_i is the Pauli σ_3 matrix acting in site i and I_f is the set of sites lying on the face. We have

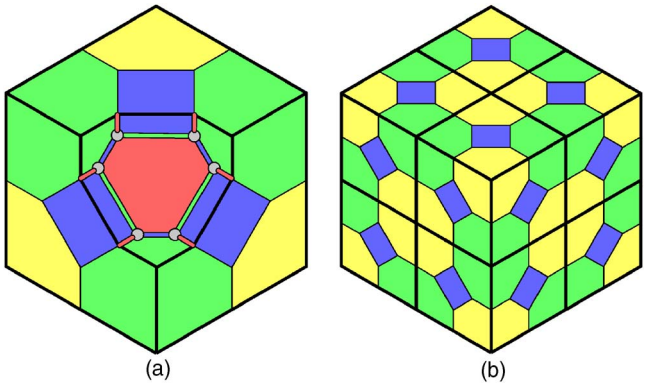

FIG. 6. (Color online) (a) The unit cell of a colex that can fill either the infinite space or a three-dimensional torus. Forgetting about colors, which are unphysical, its symmetries are those of the cube, with a single r cell at its core. Here, colors have been given both to cells and to links. A yellow cell was removed to show the interior of the unit cell. (b) Eight unit cells put together. Recall that color is not reflected in the Hamiltonian, so that all unit cells are equal although they look different due to the coloring.

$$\forall c \in C, f \in F, \quad [B_c^X, B_f^Z] = 0. \tag{3}$$

To show this, consider any cell c and face f. The edges of c come in three colors and the edges of f in two. Thus, they have at least a common color, say, q. Given any shared vertex, we consider its q-edge e. But e lies both on c and on f, and thus its other end point is also a shared vertex. Therefore, c and f share an even number of vertices and $[B_c^X, B_f^Z] = 0$.

The Hamiltonian that we propose is constructed by combining cell and face operators:

$$H = -\sum_{c \in C} B_c^X - \sum_{f \in F} B_f^Z. \tag{4}$$

Observe that color plays no role in the Hamiltonian; rather, it is just a tool we introduce to analyze it. In Appendix C, we calculate the degeneracy of the ground state. It is 2^k with

$$k = 3h_1, \tag{5}$$

and therefore depends only on the manifold, which is a sign of topological quantum order.

The ground states $|\psi\rangle$ are characterized by the conditions

$$\forall c \in C, \quad B_c^X |\psi\rangle = |\psi\rangle, \tag{6}$$

$$\forall f \in F, \quad B_f^Z |\psi\rangle = |\psi\rangle \tag{7}$$

for cell and face operators. Those eigenstates $|\psi'\rangle$ in which any of the conditions is violated are excited states. There are two kinds of excitations. If $B_c^X|\psi'\rangle = -|\psi'\rangle$, we say that there is an excitation at cell c. Similarly, if $B_f^Z|\psi'\rangle = -|\psi'\rangle$, then the face f is excited. Below, we will show that cell excitations are related to quasiparticles and face excitations to certain fluxes. For now, we are just interested in noting that excitations have a local nature and thus the Hamiltonian (4) is gapped. Then, since the ground-state degeneracy depends on the topology, we have a topological quantum order.

In order to look at our models with a broader perspective, let us briefly recall the notion of a lattice gauge theory (LGT) in the Hamiltonian formalism (space=discrete; time =continuous) to see if our lattice Hamiltonians given by Eq. (4) and higher-dimensional extensions [Eq. (27) in Sec. IV] do not fit directly into a standard LGT framework.

(a) In a LGT, the gauge degrees of freedom are located at the edges (links) of the lattice, while the gauge symmetry transformations are local operators defined at the sites (vertices) of the lattice. This is not the case for our lattices that we call D-colexes (or colexes for short) since our spin-1/2 degrees of freedom are located at the site of the colexes. Although this is not a big obstacle is defining a LGT in this setting, it is related to the major difference that we will point out next.

(b) The Hamiltonian in a LGT is constructed out of face operators (magnetic part) and site operators (electric part). This is not the case for our Hamiltonians. For example, the Hamiltonian in Eq. (4) has two contributions: one is made up of face operators B_f^Z, which fall into the class of LGT terms, and the other one is made up of cell operators B_c^X, which are not pure face operators. In fact, the X part of H cannot be written as a sum of single face or plaquette operators; in-

stead, it can be written as a sum of products of face operators, which is something different from a standard LGT.

For models in higher dimensions such as in Eq. (27), the difference is even more notorious since it may also apply to the Z part of our Hamiltonians.

It is true that our models have a certain degree of gauge symmetry since we can define local operators acting on faces (plaquettes) that commute with the Hamiltonian in Eq. (4). These operators would be analogous to the gauge transformations acting locally at the sites of a standard LGT. In our case, each face operator B_f^Z commutes with H. However, we see that our models go beyond the standard LGT.

In summary, in our models there are two main ingredients: one is the lattice structure we call colexes and the other one is the choice of X and Z terms in the Hamiltonian. Playing with these ingredients, we may find interesting physics in different dimensions D.

We would like to mention that knowing the gauge group in a LGT does not tell us everything about the physics of the model. In this regard, we look at our Hamiltonians not only as models in condensed-matter physics but also as models in quantum information.

The best way to show this is with one explicit example that we have introduced in Ref. 40. Here, we constructed two Hamiltonians, say, H_1 and H_2, in $D=2$. This time, both X- and Z-terms were face or plaquette terms for both Hamiltonians, as in a standard LGT. Also, both Hamiltonians were defined in 2-colexes with the same coordination number 3 (trivalent lattices). The difference was that for H_1 the 2-colex was a honeycomb lattice, while for H_2 the 2-colex was a mixed square-octagonal lattice.

The outcome of our study is that the quantum information capabilities of each Hamiltonian are different. The technical results can be found in Ref. 40. To be specific, H_1 does not allow us to implement the set of gates of the Clifford group, while H_2 does allow us to implement it. The benefit of this is enormous since with H_2 we can do a lot of interesting tasks altogether: quantum distillation, quantum teleportation, and quantum dense coding. In summary, the knowledge of the gauge group (when it applies) does not fix the full physical content of a given lattice Hamiltonian in certain aspects.

C. Strings and membranes

From this point on, we shall pursue a better understanding of both the ground-state degeneracy and the excitations by means of the introduction of string and membrane operators. In this direction, an essential notion will be that of a *shrunk complex*, both of the first and the second kind. The motivation after the construction of these complexes from the colexes is that only at the shrunk complex level is it possible to visualize neatly the strings and membranes that populate the model. These new shrunk complexes are not colexes, but their cells are associated with cells in the colex, and thus have color labels.

1. Shrunk complex of the first kind

The shrunk complex of the first kind is associated with a color, and it allows one to visualize strings of that particular color. Consider, for example, the b-shrunk complex. The idea is that we want to keep only the b edges, whereas the g, r, and y edges get shrunk and disappear. To this end, we start by placing a vertex at each b cell and by connecting them through edges, which are in one to one correspondence with the b edges. Then, we have to place the faces of the new complex, and they correspond to the rg, ry, and gy faces. In particular, consider a rg face. It has b and g edges, but after the g edges are shrunk, only the b edges remain. Finally, we need cells. They come from g, r and y cells. In particular, consider a g cell. It has r, y, and b edges, but only the b edges are retained. Similarly, it has gb, gr, and gy faces, but we keep only the gb faces [see Figs. 7(c) and 8 for examples].

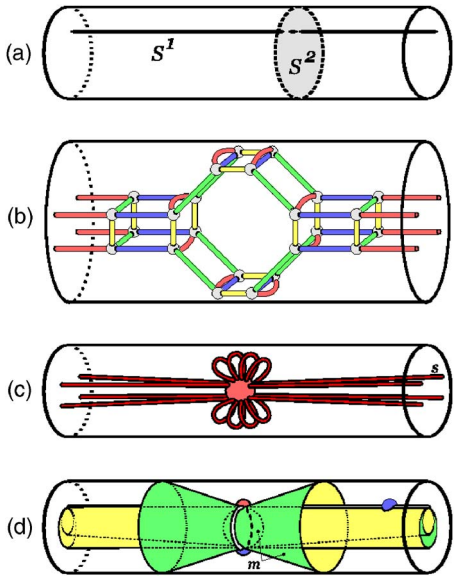

FIG. 7. (Color online) (a) A representation of the space $S^2\times S^1$. Each section of the solid tube is a sphere, and both ends of the tube are identified. (b) A 3-colex in $S^2\times S^1$. It consists of 24 vertices, twelve edges of each color, four br faces, eight by faces, six rg faces, four ry faces, four gy faces, two b cells, one r cell, three g cells, and two y cells. (c) The r-shrunk complex of the previous colex. The vertex corresponds to a r cell, and edges to r edges. An example of a closed string is the edge marked with an s. It has nontrivial homology. (d) The gy-shrunk complex of the previous colex. Vertices correspond to b and r cells, edges to rb faces, face to gy faces, and cells to g and y cells. An example of a closed membrane is a combination of the faces marked with an m. This membrane has nontrivial homology.

Now consider any path, closed or not, in the b-shrunk complex. We call such a path a b string. Recall that each edge of a shrunk complex corresponds to a b edge in the 3-colex. Thus, at the colex level, a b string is a collection of b edges that connect b cells [see Fig. 8(a)]. Each b edge contains two vertices. Then, to each b-string s, we can associate an operator $B_s^Z=\otimes_{i\in I_s}Z_i$, where I_s is the set of vertices lying in the string.

As shown in Fig. 8(b), the operator B_f^Z of a yr face corresponds to a closed b-string s. This string is the boundary of the corresponding face in the b-shrunk complex. As an operator, B_s^Z clearly commutes with the Hamiltonian and acts trivially on the ground state (6).

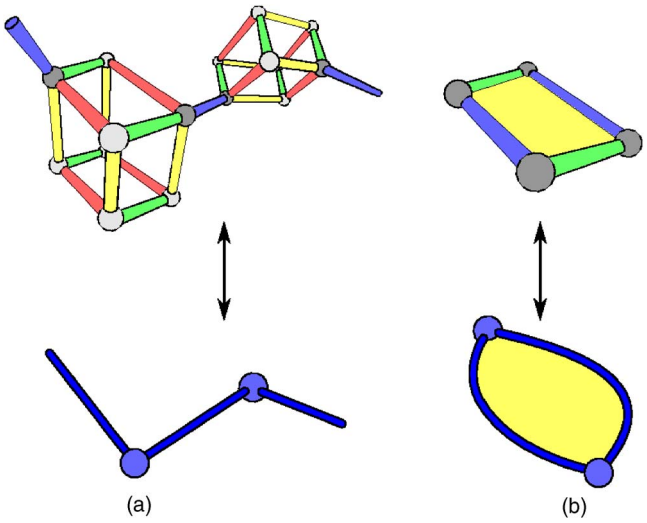

FIG. 8. (Color online) In this figure, the top represents part of a colex, and the bottom the corresponding portion of the b-shrunk complex. Vertices in the b-shrunk complex come from b-cells in the colex, edges from b-edges, faces from ry-, rg-, and gy-faces, and cells from r-, y-, and g-cells. (a) A b-string. In the colex, it is a collection of b-edges linking b-cells. In the b-shrunk complex, the path of edges can be clearly seen. (b) A ry-face corresponds to a face in the b-shrunk complex, and thus its boundary can be viewed as a b-string.

In fact, any closed string gives rise to a string operator that commutes with the Hamiltonian (4). If the string is homologous to zero, the corresponding string operator acts trivially on the ground state. In order to understand this, consider a closed red string homologous to zero. It must be a combination of boundaries of faces. Then, the string operator is the product of the operators of these faces. Similarly, the actions of two string operators derived from homologous strings of the same color are identical on the ground state. Therefore, it makes sense to label the string operators as S_μ^p, where p is a color and μ is a label denoting the homology of the string.

2. Shrunk complex of the second kind

The shrunk complex of the second kind is associated with two colors, and it allows the visualization of certain membranes, as we explain now. Let us consider, for example, the ry-shrunk complex. The idea is that we want to keep only the ry faces, whereas the rest of the faces get shrunk and disappear. This time, vertices correspond to b and g cells. Edges come from bg faces. A bg face lies between a g and a b cell, and the corresponding edge will connect the vertices coming from these cells. We have already mentioned that the faces of the ry-shrunk complex come from the ry faces in the colex, but we have to explain how they are attached. Observe that each ry face has a certain amount of adjacent gb faces. Here, for adjacent objects, we only mean that their intersection is not empty. In particular, there is a gb face at each of the vertices of the ry face. Then, the face in the complex has in its perimeter the edges coming from its adjacent gb faces. Finally, we have to consider cells, which come from r and y cells, and only keep their ry faces. So, in the boundary of a cell coming from a r cell, we see vertices from adjacent b and g cells, edges from adjacent bg faces, and faces from ry faces in the boundary of the r cell [see Figs. 7(d) and 9].

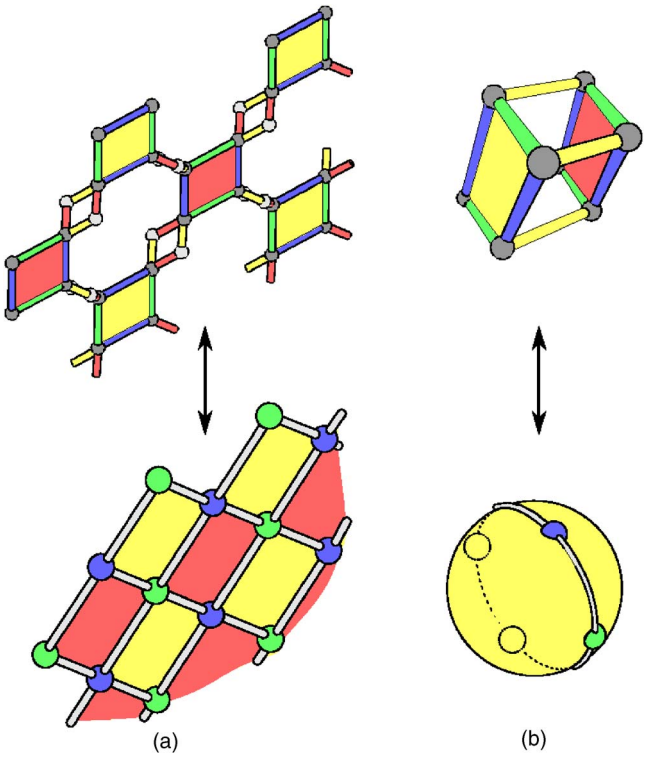

FIG. 9. (Color online) In this figure, the top represents part of a colex, and the bottom the corresponding portion of the ry-shrunk complex. Vertices in the ry-shrunk complex come from g and b cells in the colex, edges from gb faces, faces from ry faces, and cells from r and y cells. (a) An ry membrane. In the colex, it is a collection of ry faces linked by gb faces. In the ry-shrunk complex, the brane can be clearly seen. (b) An r cell corresponds to a cell in the ry-shrunk complex, and thus its boundary can be viewed as a ry membrane.

Now consider any membrane, that is, a connected collection of faces, closed or with a boundary, in the ry-shrunk complex. We call such a membrane m an ry membrane [see Figs. 7(d) and 9(a)]. We can associate an operator B_m^X with it. It is the product of the B_f^X operators of the corresponding ry faces in the colex.

As shown in Fig. 9(b), the operator B_c^X of an r-cell c corresponds to a closed ry-membrane m. This membrane is the boundary of the corresponding cell in the ry-shrunk complex. As an operator, B_m^X clearly commutes with the Hamiltonian and acts trivially on the ground state (7).

In complete analogy with strings, any closed membrane gives rise to a membrane operator that commutes with the Hamiltonian. If the membrane is homologous to zero, then the corresponding membrane operator acts trivially on the ground state. Similarly, the actions of two string operators derived from homologous membranes of the same color are identical on the ground state, and we label membrane operators as M_μ^{pq}, where p and q are colors and μ is a label denoting the homology of the membrane.

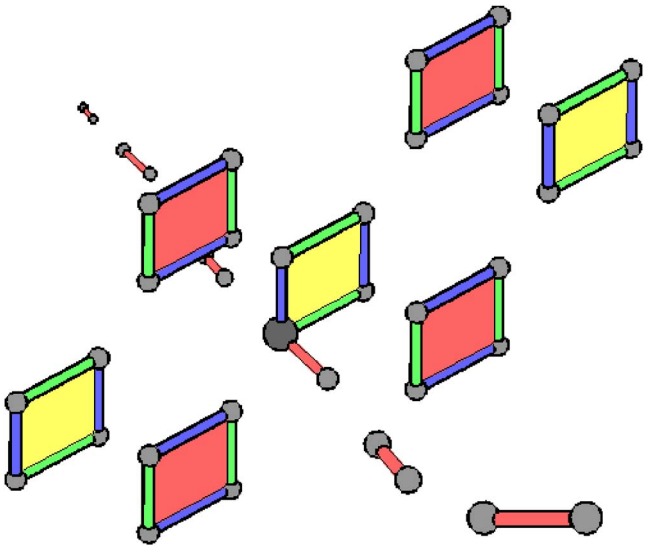

FIG. 10. (Color online) When an r string s crosses an ry membrane m, they meet at a vertex. In terms of string and membrane operators, this means that B_m^X and B_s^Z act in a common site.

3. Commutation rules

We will now consider the commutation rules between string and membrane operators. We first consider the case of a membrane and a string with no common color in their labels. As displayed in Fig. 9(a), a rg-membrane is made up of g and b edges. Then, for the same argument of Eq. (3), we have

$$\forall \mu, \nu, \quad [M_\mu^{rg}, S_\nu^b] = 0, \tag{8}$$

and analogously for any combination of three different colors. More interesting is the case in which there is a shared color. As displayed in Fig. 10, at each place where a p-string crosses a pq-membrane, they have a site in common. Thus, if the labels μ and ν are such that a ν string crosses a μ membrane an odd number of times, we have

$$\{M_\mu^{pq}, S_\nu^p\} = 0. \tag{9}$$

In another case, that is, if they cross an even number of times, the operators commute.

D. Ground state

We have discussed above how the action of string or membrane operators on the ground state depends only on their homology. It is in this sense that homologous strings or membranes give rise to equivalent operators. This equivalence, however, can be extended to take color into account, and we say that two membrane or string operators are equivalent if they are equal up to combinations with cell and face operators. Then, as we prove for general D in Appendix B, we have the following interplay between homology and color:

$$S_\mu^r S_\mu^g S_\mu^b S_\mu^y \sim 1, \tag{10}$$

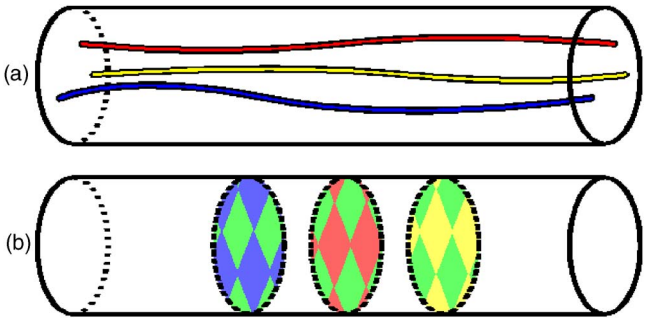

FIG. 11. (Color online) Here, we represent $S^2 \times S^1$ as in Fig. 7. In (a), a basis for nontrivial closed strings is shown. The other possible such string is green, but it is a combination of these ones (10). (b) A membrane basis in $S^2 \times S^1$. We have chosen a gb, a gr, and a gy membrane. There are three other nontrivial membranes, in particular, a br, a by and a yr membrane, but they are combinations of these ones (11).

$$M_\mu^{pq} M_\mu^{qo} M_\mu^{op} \sim 1, \tag{11}$$

where o, p, and q are distinct colors.

If we take all the r, g, and b strings for a given homology basis of 1-cycles, we obtain a complete set of compatible observables for the ground-state subspace: any other string operator is equivalent to a combination of these strings, and no membrane operator that acts nontrivially in the ground state can commute with all of them. This is, in fact, why number 3 appears in Eq. (5). As an example, a string basis in $S^2 \times S^1$ is displayed in Fig. 11(a).

Similarly, if we take all the ry, gy, and by membranes for a given homology basis of 2-cycles, we obtain a complete set of compatible observables for the ground-state subspace: any other membrane operator is equivalent to a combination of these membranes, and no string operator that acts nontrivially in the ground state can commute with all of them. A membrane basis in $S^2 \times S^1$ is displayed in Fig. 11(b).

Observe that only those string operators that have nontrivial homology, that is, which act in a global manner in the system, are capable of acting nontrivially in the ground state while living it invariant. This is the signature of a string condensate, as introduced in Ref. 49. Then, it would be tempting to let S_b be the set of all boundary strings and to try to write a ground state as

$$\sum_{s \in S_b} B_s^Z |\rightarrow\rangle^{\otimes |V|}, \tag{12}$$

where $|\rightarrow\rangle^{\otimes |V|}$ is the state with all spins pointing to the positive x direction. However, this fails. In fact, what we have is a *string-net condensate*[47] because, as indicated by Eq. (10), we can have branching points in which one string of each color meet. This means that the ground state is a superposition of all possible nets of strings, as depicted in Fig. 12. The correct way to write an example of a ground state is

$$\sum_{f \in F} (1 + B_f^Z) |\rightarrow\rangle^{\otimes |V|} =: \sum_{\text{string nets}} B_s^Z |\rightarrow\rangle^{\otimes |V|}. \tag{13}$$

We can state all of the above also in the case of membranes, and thus we should speak of a *membrane-net con-*

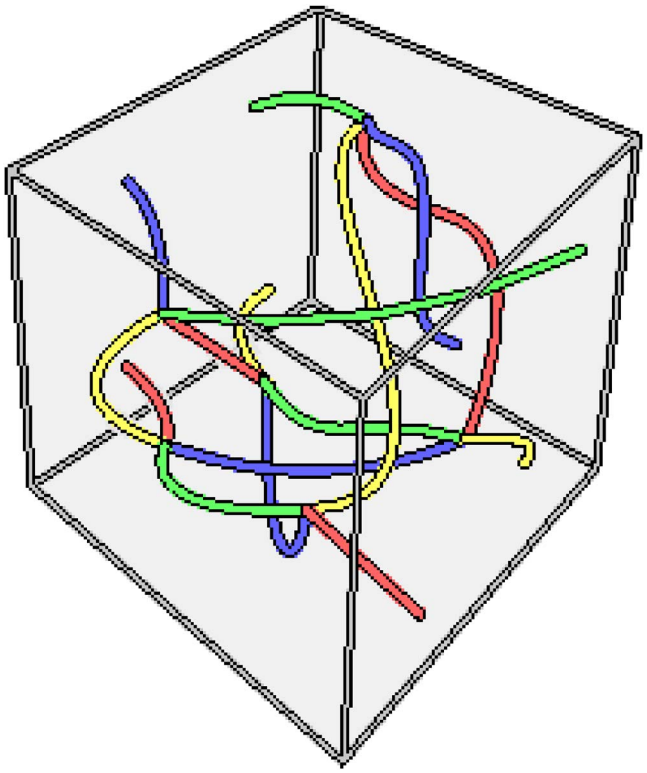

FIG. 12. (Color online) The ground state of the system is a string-net condensate. This picture represents in a 3-torus a typical element of the summation (13).

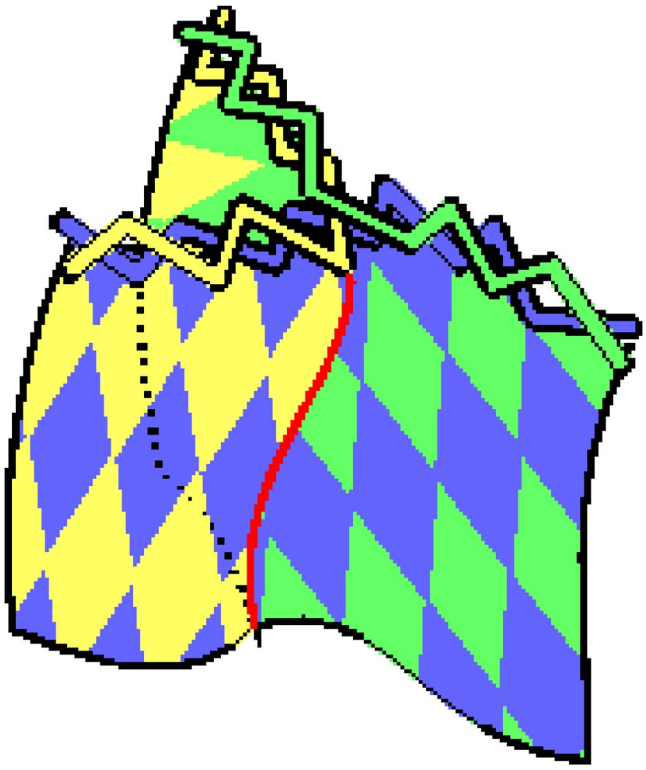

FIG. 13. (Color online) In a membrane net, different membranes can connect along common boundaries. This is related to the preservation of flux, as shown in this figure.

densate. An example of this is shown in Fig. 13. Interestingly enough, other topological orders in $D=3$ based on toric codes do not exhibit a condensation of membrane-nets.[49] It is a membrane condensate because only membranes with nontrivial homology can act nontrivially in the ground state. It is also a net because, for example, as indicated by Eq. (11), a gr, a gb, and a br membrane can combine along a curve. Then, if we let $|\uparrow\rangle^{\otimes|V|}$ denote the state with all spins up, the following is an example of a ground state:

$$\sum_{c\in C}(1+B_c^X)|\uparrow\rangle^{\otimes|V|} =: \sum_{\text{membrane nets}} B_m^X|\uparrow\rangle^{\otimes|V|}. \tag{14}$$

E. Excitations

We now focus on excitations from the point of view of string and membrane operators. We can have two kinds of excitations, depending on whether a cell or a face condition is violated. We start by considering excitations in r cells, for example. Let $|\psi\rangle$ be a ground state and S_{ij}^r an open string operator connecting the cells i and j. The state $S_{ij}^r|\psi\rangle$ is an excited state. The excitations live precisely at cells i and j, and we call them quasiparticles with an r-charge. Why should color be considered a charge? We have the following three constraints:

$$\prod_{c\in C_r} B_c^X = \prod_{c\in C_g} B_c^X = \prod_{c\in C_b} B_c^X = \prod_{c\in C_y} B_c^X, \tag{15}$$

where C_p is the set of p cells. They imply that the number of quasiparticles of each color must agree in their evenness or oddness. Therefore, if we want to create quasiparticles of a single color from the vacuum, we must create them in pairs, and so such a creation can be performed with an open string operator. Alternatively, four quasiparticles, one of each color, can also be created locally [see Fig. 14(b)]. For example, let $|\psi\rangle$ be a ground state and i any site. Then, the state $Z_i|\psi\rangle$ is a state with four quasiparticle excitations, one at each of the 3-cells that meet at site i. Observe that Eq. (15) is in agreement with Eq. (10).

Now let $|\psi\rangle$ be a ground state and M_b^{gy} a membrane operator which has a boundary ∂b. Recall that ∂b is a set of edges in the gy-shrunk complex that corresponds to a set of rb faces at the colex level. The state $M_b^{gy}|\psi\rangle$ is an excited state with excitations placed at the faces in ∂b. The excited segments, as viewed in the gy-shrunk complex, form a closed path. This introduces the idea of a gy flux in the boundary of the membrane, as illustrated in Fig. 15, for a

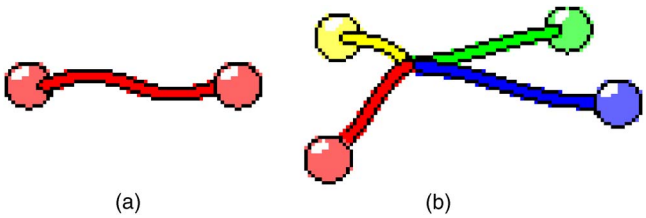

FIG. 14. (Color online) There are two ways in which quasiparticles can be created locally. We can create them either (a) by pairs of the same color forming a string or (b) in groups, one of each color forming a string net.

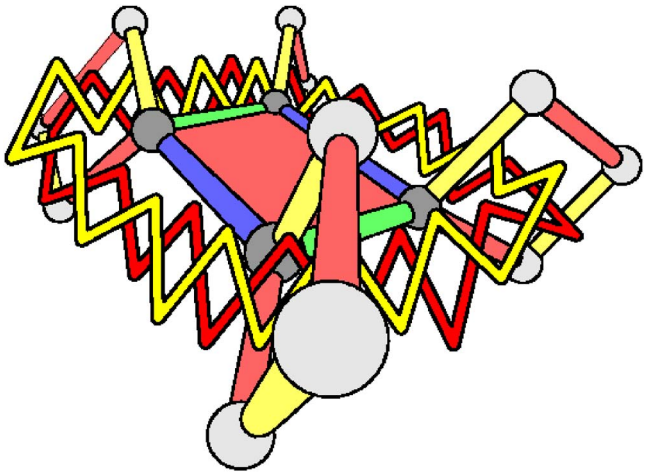

FIG. 15. (Color online) The flux excitation created with the membrane operator B_m^X of an ry membrane made up of a single ry face.

membrane with a single face. However, we have to check that this flux makes sense. Not only must it be conserved at any vertex in the gy-shrunk graph, but the existence of fluxes of other colors must also be considered. So take, for example, r-cell c. We have two constraints for the faces of c, analogous to those in Eq. (15) but in the subcolex that forms the boundary of c:

$$\prod_{f\in F_{rb}^c} B_f^Z = \prod_{f\in F_{rg}^c} B_f^Z = \prod_{f\in F_{rb}^c} B_f^Z, \tag{16}$$

where F_{pq}^c is the set of pq faces of cell c. These constraints guarantee that the gy flux is preserved at the corresponding vertex in the gy-shrunk complex. Additionally, Eq. (16) implies that a gy flux can split into a gb flux and a yb flux [see Fig. 16(b)]. This is, of course, in agreement with Eq. (11).

Fluxes can be analyzed from a different point of view. Let $|\psi\rangle$ be a ground state and i any site. Then the state $X_i|\psi\rangle$ is an excited state. We can visualize it as small p fluxes winding around the p edges incident at i, as shown in Fig. 16(c). Observe that the idea of a pq flux as something composed of a p flux and a q flux is also suggested by the flux splitting (16). Any flux configuration is a combination of these microfluxes at sites. In particular, the total flux through any closed surface must be null, and thus we cannot have, for example, an isolated rg flux in a loop which is not homologous to zero.

F. Winding quasiparticles around fluxes

In the theory of a topological order in two dimensions, it is known that quasiparticles show special statistics:[52,53] when a charge is carried around another one, sometimes the system gets a global phase, a behavior which bosons and fermions do not show. Which is the analogous situation in 3D? We can carry a charged particle along a closed path, which winds around a loop of flux, as in Fig. 17. If the system gets a global phase, then it makes sense to introduce the notion of branyons as the higher-dimensional generalization of the

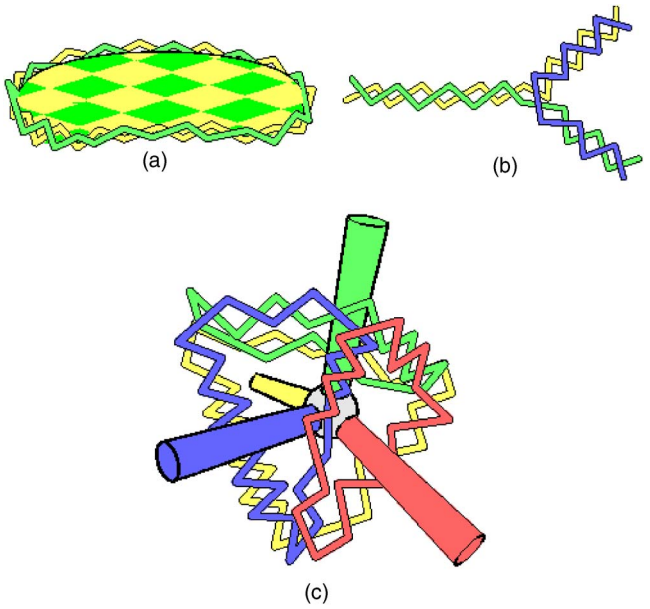

FIG. 16. (Color online) (a) The border of a gy membrane is a gy flux. (b) A gy flux can split into a gb flux and a by flux when it goes across an r cell (16). (c) The microfluxes at a given site, as explained in the text.

usual anyons. Thus, in the system at hand, we have 0-branyons (quasiparticles) and 1-branyons (fluxes). Higher-dimensional branyons will appear when we consider systems with $D \geqslant 4$.

In order to see the effect of winding a color charge around a color flux, we have to consider the closed string operator associated with the charge path and the membrane giving rise to the flux loop. If a p charge winds once around a pq flux, the system will get a global -1 phase because $\{M^{pq}, S^p\}=0$. Observe that this reinforces the idea of a pq flux as a composition of a p flux and a q flux. Other color combinations, i.e., those in which the string and the membrane do not share a color, give no phase.

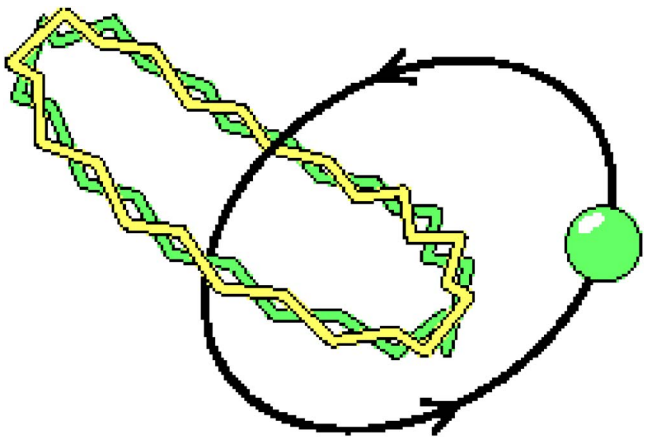

FIG. 17. (Color online) When a g charge winds around a loop of a gy flux, the system gets a global -1 phase. This is because the membrane operator giving rise to the flux and the string operator associated with the winding anticommute.

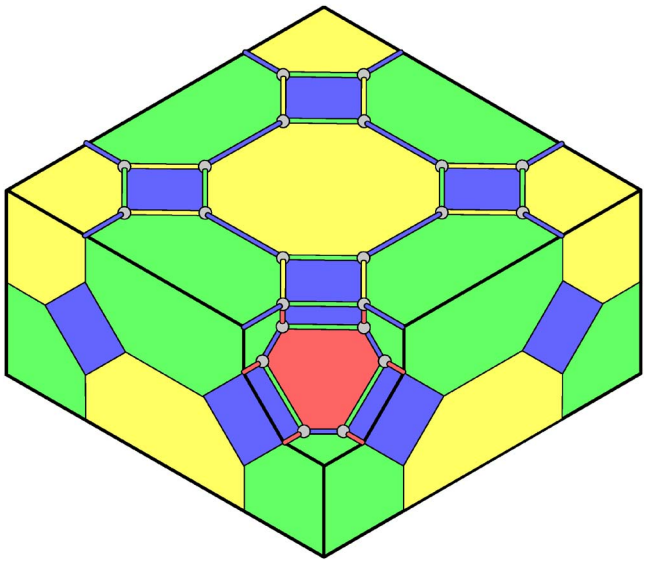

FIG. 18. (Color online) An example of a red surface, located at the boundary between the 3-colex and an erased big r cell. At a red surface, r strings can have end points without quasiparticles, and bg, gy, and by membranes can have borders without fluxes. These quasiparticles and fluxes would live precisely in the red cell that is missing. Note that a y cell was removed in the figure.

G. 3-manifolds with boundary

Up to this point, we have only considered systems contained in closed 3-manifolds. This is rather unphysical since such systems fill the whole space in which they exist, whereas any system that we can manipulate must be confined to a certain piece of space, and thus must have a boundary.

Fortunately, it is very easy to obtain manifolds with boundary from closed ones. In particular, it is enough to make holes. For example, by puncturing a 3-sphere, one obtains the usual three-dimensional Euclidean space. Of course, instead of erasing a single point, we can also remove open subsets. For example, by erasing an open ball from the 3-sphere, we get a closed ball.

How do we perform such erasures of open subsets in the case of 3-colexes? The most natural approach is to remove a certain number of cells and also all the vertices and edges that are not contained in any of the remaining cells. In doing so, we will certainly change the degeneracy of the ground state. For example, consider the 3-sphere, which gives no degeneracy. If we remove a pair of r cells, the resulting space is topologically equivalent to a thick spherical shell. In the new colex, r strings that connect both missing r cells will commute with the Hamiltonian, giving a twofold degeneracy. In general, after such a removal of cells, the new manifold will show several surfaces. We can attach a color to the surfaces, in particular, that of the cell that was removed to give that portion of the surface. Then, at a red surface, for example, r strings can have end points and bg, gy, and by membranes can have borders, whereas they still commute with the Hamiltonian. Figure 18 shows an example.

III. D COLEXES

In order to generalize the three-dimensional model to a higher dimension D, first we have to construct the underlying structure. That is, we want to define color complexes of arbitrary dimension. This section is devoted to the definition and basic properties of D colexes.

A. Definitions

First, we define color graphs or *c graphs*. A v-valent c graph is a graph Γ satisfying the conditions that (i) v edges meet at every vertex, (ii) edges are not loops, and (iii) edges are v colored. We mean by v colored that labels from a color set $Q=\{q_1,\ldots,q_v\}$ have been assigned to edges in such a way that two edges meeting at a vertex have different colors. This is a generalization of what we already saw in the $D=3$ case, as in Fig. 4. A c graph Γ' with color set Q' is a c subgraph of Γ if $\Gamma'\subset\Gamma$, $Q'\subset Q$, and the colorings coincide in common edges.

Now we introduce *complexes*. One can give to a D manifold a combinatorial structure by means of what is called a D complex. The idea is to divide the manifold in a hierarchy of objects of increasing dimension: points, edges, faces, solid spheres, etc. These objects are called n cells, $n=0,\ldots,D$. 0-cells are points, 1-cells are edges, and so on. The boundary of an n cell is an n sphere and is made up of cells of dimension $n'<n$. So, what we have is a D manifold constructed by gluing together the higher-dimensional analogs of the polyhedral solids that we considered in $D=3$ (recall Fig. 2).

A D colex is a complex in a D manifold which has $(D+1)$-colored edges in such a way that (i) its underlying lattice or graph is a $(D+1)$-valent c graph, (ii) the subgraph that lies on the boundary of any n cell for $n=2,\ldots,D$ is an n-valent c subgraph, and (iii) any connected c subgraph with valence $v=2,\ldots,D$ lies on the boundary of one unique v cell. Therefore, the point is that the c graph *completely* determines the cell structure and thus the whole topology of the manifold.

Some c graphs yield a colex, but not all of them. We define recursively this partially defined mapping from the space of $(D+1)$-valent c graphs to the space of closed D manifolds. First, any 2-valent c graph is a collection of loops. So, as a topological graph, it naturally yields a 1-manifold, namely, a collection of 1-spheres. Then, consider any 3-valent c graph. We construct a 2-complex starting with the corresponding topological graph or 1-complex. The idea is to list first all 2-valent c subgraphs, which are embeddings of S^1 in the 1-complex. Then, for each of these subgraphs, we attach a 2-cell, gluing its boundary to S^1. The resulting space is certainly a 2-manifold. It is enough to check a neighborhood of any vertex, but the one to one correspondence between cells and connected c subgraphs makes this straightforward. Then, we consider a 4-valent c graph. If not all of its 3-valent c subgraphs yield S^2, we discard it. Otherwise, we first proceed to attach 2-cells as we did for the 3-valent graph. Then, we list all 3-valent c subgraphs, which by now correspond to embeddings of S^2 in a 2-complex. At each of these spheres, we glue the surface of a solid sphere. The process can be continued in an obvious way, and thus in general a $(D+1)$-valent c graph yields a D colex if and only if all its D-valent c subgraphs yield S^D.

B. Examples

As a first example of a colex, consider the c graph composed of only two vertices, for any valence $v=D+1\geqslant 2$. An

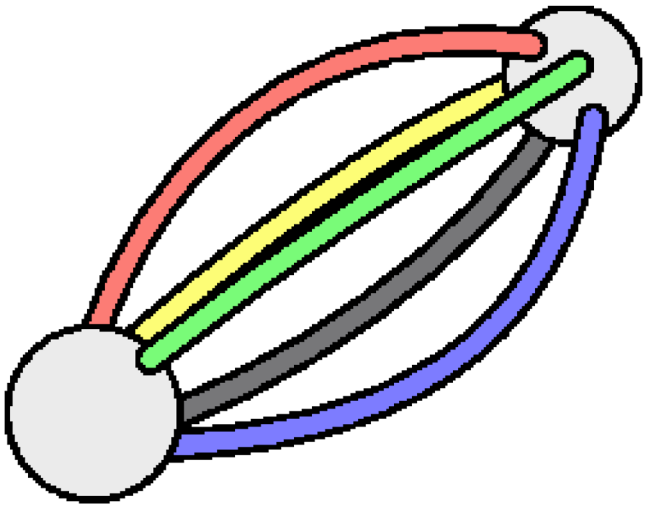

FIG. 19. (Color online) A c graph that yields a 4-sphere. It is the simplest possible 4-colex, with only two vertices.

example can be found in Fig. 19. This family of c graphs yields the spheres S^D. This can be visualized by viewing S^D as $\mathbf{R}^D$ plus the point at infinity. We can place one vertex at the origin and the other at infinity. Then, edges are straight lines that leave the origin in different directions.

The projective space P^D can also be described easily with a colex, though less economically in terms of vertices. Recall that P^D can be constructed by identifying opposite points of the boundary of a D-dimensional ball. The idea is to consider a D cube and to construct a D-valent c graph with its vertices and edges, coloring parallel edges with the same color. Then, we add 2^{n-1} extra edges to connect opposite vertices, and we give them a new color. The resulting c graph yields P^D. See Fig. 5 for an example of the case $D=3$.

In Appendix A, we give a procedure to construct colexes from arbitrary complexes. This guarantees that we can construct our topologically ordered physical system in any closed manifold with $D \geqslant 2$.

C. *R*-shrunk complex

This section is devoted to the construction of several new complexes from a given colex. These constructions will be essential to the understanding of the physical models to be built. In particular, as we learned in the $D=3$ case, only at the shrunk complex level will it be possible to visualize neatly the branes that populate the system. Shrunk complexes also provide us with several relations among the cardinalities of the sets C_n of n cells, which in turn will be essential in calculating the degeneracy of the ground state. These relations are based on the Euler characteristic of a manifold, a topological invariant defined in a D complex as

$$\chi := \sum_{n=0}^{D} (-1)^n |C_n|. \tag{17}$$

Before starting with the construction, it is useful to introduce the notion of the Poincaré dual of a complex $\mathcal{C}$ in a D manifold. The dual complex $\mathcal{C}^*$ is obtained by transforming the n cells of $\mathcal{C}$ in $(D-n)$ cells and by inverting the relation being-the-boundary-of. This means that if a certain $(n-1)$ cell c' is in the boundary of the n cell c in $\mathcal{C}$, then c^* is in the boundary of c'^* in $\mathcal{C}^*$.

We say that a cell is a R-cell if its c graph has as color set R. Note that this notation is different from the one we used in $D=3$, but it is more suitable for high D. What was before a gy membrane will now be a $\{r,b\}$ brane, or more simply a br brane, and so on.

Consider a D colex $\mathcal{C}$ with color set Q. We want to construct its R-shrunk complex $\mathcal{C}_R$, where R is a nonempty proper subset of Q, $\emptyset \subsetneq R \subsetneq Q$. What we seek is a new complex in which only R-cells remain, whereas the rest of the $|R|$-cells disappear. This construction is accomplished by a partial Poincaré dualization of cells. We already saw examples of this construction in $D=3$. Due to the different notation, what was called a gy-shrunk complex now will be called a rb-shrunk complex.

The R-shrunk complex has two main sets of cells. The first one corresponds to the cells in the set

$$S_1 := \bigcup_{R \subseteq S \subsetneq Q} C_S, \tag{18}$$

where C_S is the set of S cells. Cells in S_1 keep their dimension and the relation being-the-boundary-of among them. The second cell set is

$$S_2 := \bigcup_{\bar{R} \subseteq S \subsetneq Q} C_S, \tag{19}$$

where $\bar{R}$ is the complement of R in Q,

$$\bar{R} := Q - R. \tag{20}$$

Cells in S_2 get dualized. This means that an n cell in the colex will be a $(D-n)$ cell in the R-reduced complex. The relation being-the-boundary-of is inverted among the cells in S_2. So, S_2 provides us with cells of dimensions $0,\ldots,|R|-1$ and S_1 with cells of dimensions $|R|,\ldots,D$. Up to dimension $|R|-1$, the construction is clear, but we have to explain how to attach the cells in S_1. To this end, we observe that the intersection of an n-cell in S_1 and an R cell is either empty or a cell of dimension $n'=n-|\bar{R}|$. The n cell gives rise to a cell of dimension $D-n=|R|-1-n'$. Thus, the partial dualization is, in fact, a complete dualization, as seen on the boundary of any R cell, and the attachment of each R cell is then naturally described by this dualization process, as shown in Fig. 20. For the cells coming from S cells with $R \subsetneq S$, the attachment can be described recursively. The boundary of these cells is a $(|S|-1)$-colex, so we can obtain its R-shrunk complex and use it as the new boundary for the cell. In fact, what we are doing is a projection of the shrinking process in the boundary of the cell. Figure 21 displays examples of shrunk complexes for $D=2$.

The Euler characteristic for a R-shrunk complex is

$$\chi = \sum_{R \subseteq S \subsetneq Q} (-1)^{|S|} |C_S| + \sum_{\bar{R} \subseteq S \subsetneq Q} (-1)^{D-|S|} |C_S|. \tag{21}$$

If we sum up all such equations for all different color combinations but for a fixed cardinality $|R|=r$, we get

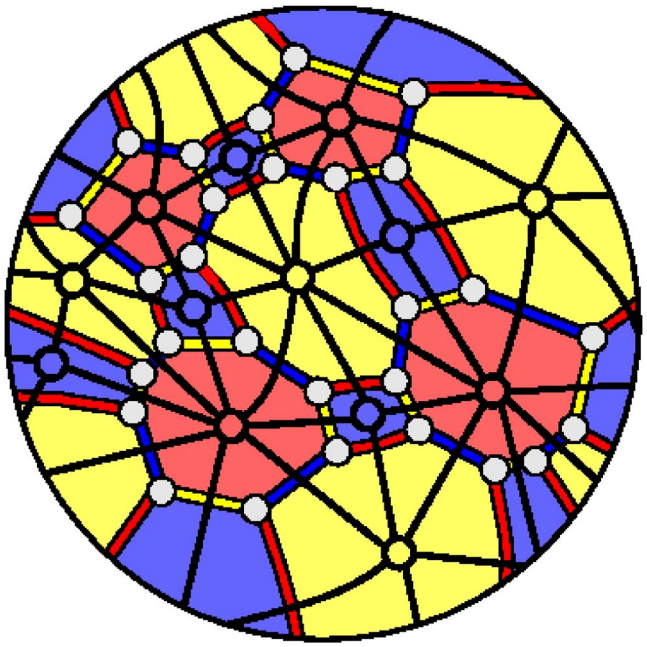

FIG. 20. (Color online) A *bry* cell belonging to some D colex with $D \geqslant 3$. We show superimposed in black thick line the structure of its dual boundary, which plays an important role when constructing the *bry*-shrunk complex.

$$\binom{D+1}{r}\chi = \sum_{n=r}^{D} (-1)^n \binom{n}{r} |C_n| + \sum_{n=0}^{r-1} (-1)^n \binom{D-n}{D-r+1} |C_{D-n}|. \tag{22}$$

The case $r=0$ is also included since it reduces to the definition of χ. The right-hand side (rhs) in the cases $r=s$ and $r=D-s+1$ are equal except for the sign, so that we get

$$\chi = (-1)^D \chi. \tag{23}$$

Of course, it is a well-known fact that χ vanishes in manifolds of odd dimension. In these cases in which $D=2k+1$, Eq. (22) for $r=k+1$ vanishes identically. So, in general, we have $\lceil D/2 \rceil$ independent relations. They tell us that the cardinalities $|C_0|, \ldots, |C_{\lfloor D/2 \rfloor}|$ depend on the cardinalities $|C_{\lfloor D/2+1 \rfloor}|, \ldots, |C_D|$, which shows quantitatively the fact that colexes are much more "rigid" than more general complexes.

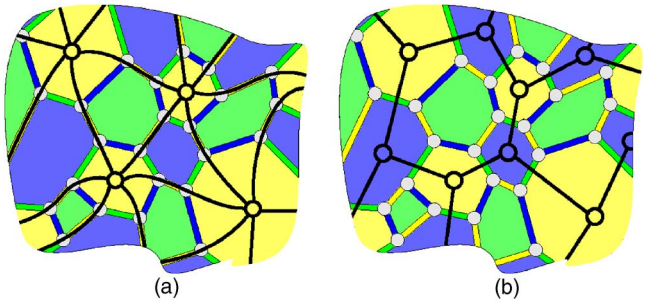

FIG. 21. (Color online) This figure shows the two possible kinds of shrunk complex in a 2-colex. The shrunk complexes appear superimposed in black thick line to the original colex. In (a), the *y*-shrunk complex is shown, and in (b) the *by*-shrunk complex.

IV. THE MODEL IN D-MANIFOLDS

A. System and Hamiltonian

We now associate a physical system with a D-colex structure in a D-manifold, $D \geqslant 2$. To this end, we place at each vertex (site) a spin-$\frac{1}{2}$ system. To each n-cell c, we can attach the cell operators

$$B_c^\sigma := \bigotimes_{i \in I_c} \sigma_i, \quad \sigma = X, Z, \tag{24}$$

where X_i and Z_i are the Pauli σ_1 and σ_3 matrices acting on the spin in the vertex i and I_c is the set of vertices lying on cell c. In order to generalize the Hamiltonian (4), we need sets of cells such that their X and Z operators commute. However, we have the following result. For every n-cell c_n and m-cell c_m with $n+m > D+1$,

$$[B_{c_n}^X, B_{c_m}^Z] = 0. \tag{25}$$

This is a consequence of the fact that c_n and c_m have colexes with at least one color in common because they have respectively $p+1$ and $(q+1)$ colors. Then, their intersection is a colex of valence of at least 1, and thus contains an even number of sites.

From this point on, we choose fixed integers $p, q \in \{1, \ldots, D-1\}$ with

$$p + q = D. \tag{26}$$

The Hamiltonians that we propose are

$$H_{p,q} = -\sum_{c \in C_{p+1}} B_c^Z - \sum_{c \in C_{q+1}} B_c^X. \tag{27}$$

Again, color plays no role in the Hamiltonian. It is an exactly solvable system, and the ground state corresponds to a quantum error correcting code with cell operators as stabilizers.[54] We give a detailed calculation of the degeneracy in Appendix C. The degeneracy is 2^k with

$$k = \binom{D}{p} h_p = \binom{D}{q} h_q, \tag{28}$$

where $h_p = h_q$ is the pth Betty number of the manifold. The ground states $|\psi\rangle$ are characterized by the conditions

$$\forall c \in C_{p+1}, \quad B_c^Z |\psi\rangle = |\psi\rangle, \tag{29}$$

$$\forall c \in C_{q+1}, \quad B_c^X |\psi\rangle = |\psi\rangle. \tag{30}$$

Those eigenstates $|\psi'\rangle$ for which some of these conditions are violated are excited states. As in the $D=3$ case, excitations have a local nature and we have a gapped system.

For $D \geqslant 4$, different combinations of the parameters (p,q) are possible. Each of these combinations gives rise to different topological orders, thus making transitions between them possible. For example, in $D=4$, the Hamiltonian

$$H = H_{1,3} + \lambda H_{2,2} \tag{31}$$

exhibits a topological phase transition as λ is varied.

The Hamiltonian in Eq. (31) is not exactly solvable, while $H(1,3)$ and $H(2,2)$ are exactly solvable separately, by construction. The reason is that the sets of face operators B_f^Z and cell operators B_c^X of type (1,3) do not commute with the corresponding sets of operators of type (2,2).

The Hamiltonian H does not have an exact topological order for arbitrary values of the coupling constant λ; only at the weak coupling $\lambda \ll 1$ or strong coupling $\lambda \gg 1$ does it show a topological order of a different type. As the coupling is varied, we connect two different topological phases, but the whole line in λ is not necessarily topological.

Now that we have seen this mechanism for producing topological quantum phase transitions with colexes in the simplest case, we can extend it to arbitrary dimensions $D \geqslant 4$ by introducing the following set of Hamiltonians:

$$H_D = \sum_{p,q:p+q=D} \lambda_{p,q} H_{p,q}, \tag{32}$$

where the Hamiltonians $H_{p,q}$ are given by Eq. (27). As the coupling constants $\lambda_{p,q}$ are varied and meet the topological points characterized by $\lambda_{p,q}=0$, $\forall p$, $q \neq p_t$, q_t, $\lambda_{p_t,q_t}=1$, we find again examples of topology-changing phase transitions.

B. Branes

In analogy with the string and membranes that appeared in the $D=3$ case, here we have to consider p branes. We mean by a p brane an embedded p manifold, closed or with a boundary. A p brane is homologous to zero when it is the boundary of a $p+1$ brane. Then, two p branes are homologous if the p brane obtained by their combination is homologous to zero.

Let Q be the set of colors of the D colex. Then, for any nonempty set $R \subsetneq Q$, a R brane is a collection of R cells. It can be truly visualized as a $|R|$-brane in the R-shrunk complex. There, we also see that its boundary corresponds to $\bar{R}$ cells. Let b be an R brane and C_b its set of R cells. Then, we can attach to b operators $B_b^\sigma := \Pi_{c \in C_b} B_c^\sigma$ for $\sigma = X, Z$. Suppose, in particular, that $|R|=p$ and let b be a closed R brane. Then, B_b^Z commutes with the Hamiltonian. If this were not the case, there would exist a $(q+1)$ cell, particularly an $\bar{R}$ cell c, such that $\{B_b^Z, B_c^X\}=0$. However, in that case, in the R-shrunk complex, the p brane would have a boundary at the cell coming from c. Similarly, closed q-brane X operators also commute with the Hamiltonian.

The operator B_c^Z of a $(p+1)$ cell c with color set $R \cup \{r\}$, $r \in Q-R$, is a closed R-brane. As the R-shrunk complex reveals, it corresponds to the boundary of c. B_c^Z acts trivially in ground states (29), and the same holds true for any closed p-brane homologous to zero since it is a combination of such operators B_c^Z. This is not the case for closed p branes, which are not homologous to zero, and thus they act nontrivially in the ground state.

1. Equivalent branes

It is natural to introduce an equivalence among those operators of the form $\otimes_{v \in V} Z_v^{i_v}$, where V is the set of vertices of the colex and $i_v \in \{0,1\}$. We say that two such operators O_1 and O_2 are equivalent, $O_1 \sim O_2$, if $O_1 O_2$ is a combination of $(p+1)$ cell operators B_c^Z. This induces an equivalence among p branes since they have such an operator attached. In fact, two R branes, b and b', with $|R|=p$, are equivalent if and only if they are homologous. Observe that two equivalent p brane Z operators produce the same result when applied to a ground state. This motivates the introduction of the notation P_μ^R, $|R|=p$, for any operator B_b^Z, with b a R brane with homology labeled by μ.

Likewise, we can introduce an equivalence among those operators of the form $\otimes_{v \in V} X_v^{i_v}$, just as we have done for Z operators. This induces an equivalence relation among q branes, and we use the notation Q_ν^R, $|R|=q$, for any q-brane operator B_b^X, with b an R brane with homology labeled by ν.

In Appendix B, we show that for any color set $R \subset Q$ with $|R|=p-1$,

$$\prod_{r \in Q-R} P_\mu^{rR} \sim 0, \tag{33}$$

where rR is a shorthand for $\{r\} \cup R$. Similarly, if $|R|=q-1$,

$$\prod_{r \in Q-R} Q_\mu^{rR} \sim 0. \tag{34}$$

These relations generalize Eqs. (10) and (11). They give the interplay between homology and color, and show that for each homology class only $\binom{D}{p}$ color combinations are independent, those which can be formed without using one of the $D+1$ colors. This is why a combinatorial number appears in the degeneracy of the ground state. The other factor, h_p, follows from the fact that a homology basis for p-branes has h_p elements. By using the theory of quantum stabilizer codes,[54] one can see that by selecting a basis for p-branes with labels $\mu=1,\ldots,h_p$ and a color r, we can form a complete set of observables $\{P_\mu^R\}_{\mu,R \ni r}$.

2. Commutation rules

In general, for suitable color sets R,S, we have

$$R \cap S \neq \emptyset \Rightarrow [P_\mu^R, Q_\nu^S] = 0. \tag{35}$$

This follows from the same reasoning used in Eq. (25). We now explore the situation when R and S have no color in common. Consider a basis $\{p_\mu\}$ for closed p-branes. Consider also a basis for q-branes $\{q_\nu\}$, chosen so that p_μ and q_ν cross once if $\mu=\nu$ and do not cross in other cases. Then,

$$R \cap S = \emptyset \Rightarrow P_\mu^R Q_\nu^S = (-1)^{\delta_{\mu,\nu}} Q_\mu^S P_\nu^R. \tag{36}$$

This can be reasoned without resorting to the geometrical picture. Suppose that $[P_\mu^R, Q_\mu^S]=0$ and let $R=R' \cup \{r\}$, $Q-R-S=\{q\}$. From Eq. (33), we have $[\Pi_{r'} P_\mu^{R'r'}, Q_\mu^S]=0$. Then, Eq. (35) implies $[P_\mu^{Rq}, Q_\mu^S]=0$, and thus we have a homologically nontrivial q-brane X operator that commutes with all the p-brane Z operators. This being impossible, the assumption is necessarily false.

C. Excitations

There are two kinds of excitations, depending on whether a $(p+1)$-cell or a $(q+1)$-cell condition is violated. We label

excitations with the color set of the cell they live in. Although we focus on the violation of $(q+1)$ cells, the situation is analogous for $(p+1)$ cells.

Let $|\psi\rangle$ be a ground state and b an R brane, $R \subset Q$, $|R|=p$. We first observe that b has a boundary in the R-shrunk complex at the cell corresponding to the $\bar{R}$ cell c if and only if

$$\{P_b^R, B_c^X\} = 0. \tag{37}$$

However, $B_b^Z|\psi\rangle$ has $\bar{R}$ excitation exactly at those cells fulfilling Eq. (37). This means that the excitation produced by the p brane b has the form of a $p-1$-brane, precisely the boundary of b, ∂b.

Consider the particular case $p=1$. The excitations living at D-cells are, as in the $D=3$ case, quasiparticles (anyons) with color charge. In a connected manifold, we have D constraints generalizing Eq. (15). They have the form

$$\prod_{c \in C_R} B_c^X = \prod_{c \in C_S} B_c^X, \tag{38}$$

where $|R|=|S|=D$ and C_R is the set of R cells. These relations imply that the number of particles of each color must agree in their parity. Therefore, from the vacuum, we can create pairs of particles of a single color or groups of $D+1$ particles, one of each color. This is completely analogous to $D=3$.

Now suppose that $p>1$. We have seen that excitations can be created as the boundary of a p brane. If, in particular, it is an R brane, then excitations live in $\bar{R}$ cells. It is natural to interpret these excitations as some kind of $(p-1)$-dimensional flux, an $\bar{R}$ branyon. Then, it must be conserved. In fact, for each $(q+2)$ cell c, we have the constraint

$$\prod_{c \in C_R^c} B_c^X = \prod_{c \in C_S^c} B_c^X, \tag{39}$$

where $|R|=|S|=q+1$ and C_R^c is the set of R cells lying on cell c. This is a generalization of Eq. (16) and is in agreement with Eq. (33).

Finally, as in the three-dimensional case, we can wind branyons around each other and sometimes get a global phase. Let $|R|=q+1$ and $|S|=p+1$. Then, when a R branyon winds around a S branyon, the system gets a global minus sign if and only if $|R \cap S|=1$, following the commutation rules (36).

V. CONCLUSIONS

In this paper, we have explored topological orders in $D=3$ by means of models for quantum lattice Hamiltonians constructed with spins $S=\frac{1}{2}$ located at lattice sites. These models are exactly solvable, and this is a feature that allows us to explore the quantum properties of the whole spectrum. The ground state is found to be in a string-net condensate or, alternatively, in a membrane-net condensate. This type of membrane-net condensation is an interesting feature of our models that does not appear in 3D toric codes. In dimensions higher than $D=3$, we have also extended the construction of our models and found brane-net condensation. As for excitations, they are either quasiparticles or a certain type of extended fluxes. These excitations show unusual braiding statistical properties similar to anyons in $D=2$, and we call them branyons since they involve extended objects associated with branes.

Another interesting result is the possibility of having a topology-changing transition between two topologically ordered phases that we find with our models in $D=4$. We may wonder whether it is possible to have a similar topology-changing process in dimension $D=3$ as in Eq. (31). One obvious way to achieve this is by using the construction in $D=4$ and flattening it into $D=3$, thereby reducing the dimensionality of the interaction but at the expense of losing the locality of the interaction.

A fully or completely topological order does not exist in $D=3$ dimensions, unlike in $D=2$. That is to say, a topological order that can discriminate among all the possible topologies in three-dimensional manifolds does not exist. We may introduce the notion of a topologically complete class of quantum Hamiltonians when they have the property that their ground-state degeneracy (and similarly for excitations) is different, depending on the topology of the manifold where the lattice is defined. From this perspective, we have found a class of topological orders based on the construction of certain lattices called colexes that can distinguish between 3D-manifolds with different homology properties. Homology is a topological invariant, but not enough to account for the whole set of topologically inequivalent manifolds in $D=3$. For instance, the famous Poincaré sphere is an example of a 3D-manifold that has the same homology as a 3-sphere. Poincaré was able to prove that the fundamental group (or first homotopy group) of this new sphere has the order 120. As the standard 3-sphere has a trivial fundamental group, it is different. Since then, many other examples of homology spheres that are different topological structures have been constructed. In this regard, we could envisage the possibility of finding a quantum lattice Hamiltonian, possibly with a non-Abelian lattice gauge theory, that could distinguish between any topology in three dimensions by means of its ground-state degeneracy. This would amount to solving the Poincaré conjecture with quantum mechanics.

From the viewpoint of quantum information, the topologically ordered ground states that we have constructed provide us with an example of topological quantum memory: a reservoir of states that are intrinsically robust against decoherence due to the encoding of information in the topology of the system.

ACKNOWLEDGMENTS

We acknowledge financial support from a PFI fellowship of the EJ-GV (H.B.), DGS grant under Contract No. BFM 2003-05316-C02-01 and INSTANS (M.A.MD.), and CAM-UCM grant under Ref. No. 910758.

APPENDIX A: HOW TO CONSTRUCT D COLEXES

We present a procedure to construct colexes in arbitrarily closed manifolds. The idea is to start with an arbitrary com-

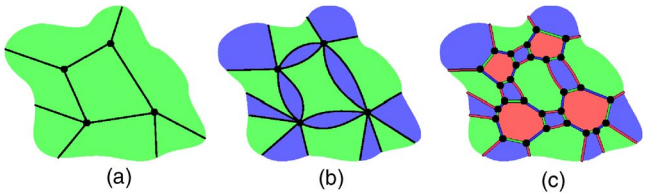

FIG. 22. (Color online) This figure explains a process that converts an arbitrary 2-complex on a surface into a 2-colex. In (a), green color is given to all the 2-cells of the 2-complex. In (b), 1-cells are inflated to give blue 2-cells. Finally, in (c), 0-cells are inflated to give red 2-cells, and 1-cells are accordingly colored.

plex and inflate its cells until a colex is obtained. We now explain the process in detail. It is illustrated in Fig. 22.

First, we have to state what we mean by inflating an n cell, $0 \leqslant n \leqslant D$. The idea is to keep the boundaries of the cell untouched but to inflate all other points in order to obtain a D-cell. For each $(n+l)$ cell that belongs to the boundary of the inflated cell, we must introduce an $(n+l-1)$ cell. The inflation of cells of the same dimension can be performed in any order, and all the cells must be inflated. Inflation starts with $(n-1)$ cells, then continues with $(n-2)$ cells, and so on, until 0-cells are inflated in the end.

We can prove that this procedure gives a D colex by an inductive argument. We will need some facts. First, we observe that the D cells of a D colex can be labeled with the unique color, which its subcolex does not contain. Conversely, if we can color the D cells of a D colex with $D+1$ colors in such a way that neighboring cells have different colors, then we can color edges according to the D cells they connect. Note also that for each cell in the original D complex, the inflated one has a D cell. This means that we can label inflated D cells with the dimension of the cell in the original complex.

Finally, we proceed with the proof. The case $D=1$ is trivial. We suppose that the procedure works for D manifolds, and we check it for $(D+1)$ manifolds. To this end, consider the boundary of any inflated $(D+1)$ cell which comes from the inflation of a 0-cell. Imagine all the inflation processes projected into this (fixed) D sphere. In the beginning, we can see a complex in this sphere. Its vertices correspond to edges that cross the surface, edges to faces that cross it, and so on. As the inflation proceeds in the original complex, the projected complex is also inflated. When 1-cells are inflated, the projected complex has become a D colex because of the induction hypothesis. Thus, it can be properly colored. Moreover, we can perform the coloring on its D cells using the labels attached to the corresponding $(D+1)$ cells in the inflated $(D+1)$ complex. From this coloring, we deduce a coloring for the edges of the D colex. In fact, all this is true for each of the subgraphs on the surfaces of $(D+1)$ cells obtained by inflation of 0-cells. Finally, we give a different color to the edges that are not contained in these surfaces. Checking that this coloring gives the desired properties that make the complex a colex is now easy.

APPENDIX B: BRANE COMBINATION

Consider a D colex with color set Q. Let b_R be a closed R brane, $\varnothing \subsetneq R \subsetneq Q$. It is the purpose of this section to show that for any $r \in R$, there exists a family of closed $|R|$ branes b_S homologous to B_R such that

$$B^{\sigma}_{b_R} = \prod_S B^{\sigma}_{b_S}. \tag{B1}$$

The sum extends over all $S \subset \bar{r} := Q - \{r\}$ with $|S| = |R|$.

We first consider the case $R=\{r\}$. Then, b_R is a string. It consists of r edges that link $\bar{R}$ cells. $B^{\sigma}_{b_R}$ acts nontrivially in an even number of vertices per $\bar{R}$ cell. Thus, we can gather them together in pairs and connect them through a path which only contains edges with colors in $Q-R$. Then, for each $s \in Q-R$, the set of all s edges we have used forms a string b_S, $S=s$. Then, certainly, Eq. (B1) holds true and each string b_S is closed because the rhs commutes with operators from $\bar{S}$ cells, and so does the left-hand side (lhs).

Now consider the case $|R|>1$. Let $\tilde{r} := R-\{r\}$. Consider the restriction of $B^{\sigma}_{b_R}$ to any $\bar{r}$-cell c, denoted as B^{σ}_{b}. This operator corresponds to a closed $\tilde{r}$ brane b in the $(D-1)$ colex that forms the boundary of c. Since this colex is a sphere, b is a boundary and thus B^{σ}_{b} is a combination of $|R|$ cells. As we did for strings, we can do this for every $\bar{r}$ cell, gather cells together by color and form the required closed $|R|$ branes.

APPENDIX C: DEGENERACY OF THE GROUND STATE

In the theory of quantum error correcting codes, the ground state of the Hamiltonian (27) is called a stabilizer code.[54] Thus, the theory of stabilizer codes naturally fits in the study of degeneracy, but we will avoid using its language although this makes the exposition less direct.

The ground state of the Hamiltonian (27) is the intersection of subspaces of eigenvalue 1 of $(p+1)$-cell and $(q+1)$-cell operators, as expressed in Eqs. (29) and (30). This subspace has an associated projector, which in turn will be the product of the projectors onto each of the subspaces of eigenvalue 1:

$$\prod_{c \in C_{p+1}} \frac{1}{2}(1 + B^{Z}_{c}) \prod_{c \in C_{q+1}} \frac{1}{2}(1 + B^{X}_{c}). \tag{C1}$$

Each of these projectors reduces the dimension of the space by half, but not all of them are independent because certain relations among cell operators exist. For $(p+1)$ cells, these relations have the form

$$\prod_{c \in C_{p+1}} (B^{Z}_{c})^{i_c} = 1, \tag{C2}$$

where $i_c = 0, 1$. Analogous relations exist for $(q+1)$ cells:

$$\prod_{c \in C_{q+1}} (B^{X}_{c})^{i_c} = 1. \tag{C3}$$

If the number of spins is n and the number of independent projectors is l, then the degeneracy of the ground state will be 2^k, with $k=n-l$. Suppose that the number of independent relations of type (C2) is l_1 and that for relations (C3) is l_2. Then, we have $l = |C_{p+1}| - l_1 + |C_{q+1}| - l_2$. Our starting point is then the equation

$$k = |C_0| - |C_{p+1}| - |C_{q+1}| + I(D,p+1) + I(D,q+1), \tag{C4}$$

where $n=|C_0|$ is the number of sites and $I(D,s)$ is the number of independent relations among s cells in a D colex.

$I(D,s)$ only depends on the cardinalities of cell sets $|C_i|$ and the Betty numbers of the manifold h_i, as we will show by calculating its value recursively. First, we note that

$$I(D,D) = dh_0 \tag{C5}$$

because the unique independent relations in this case are those in Eq. (38), for each connected component. For $s<D$, a relation between cells has the general form

$$\prod_{|S|=s} \prod_{c \in D_S} B_c^\sigma = 1, \tag{C6}$$

where $D_S \subset C_S$. Let $r \in Q$ be a color. If we only consider those relations that include color sets $R \subset \bar{r}$, we effectively reduce the problem by one dimension. By gathering together all such relations that appear in $\bar{r}$ cells, we get a total count of

$$I_{\bar{r}}(D,s) = I(D-1,s)\big|_{h_0=h_D=|C_{\bar{r}}|, h_{i\neq 0,D}=0}. \tag{C7}$$

Since the rhs of Eq. (C6) commutes with any cell operator, the relation has the form

$$\prod_{|S|=s} B_{b_S}^\sigma = 1, \tag{C8}$$

where b_S is a *closed* S-brane b_S. Then, consider any such relation in which a R-brane b_R appears with $r \in R$. If we have at hand all the relations of the form (B1), we can use them to eliminate the term b_R in Eq. (C8). This can be done for every such R, until a relation containing only colors in $\bar{r}$ is obtained. Therefore, our next task is to count how many of the relations (B1) are independent for each R.

Suppose then that we have a relation of the form (B1) that follows from other t relations of the same form (but not from a subset of them):

$$B_{b_{R,i}}^\sigma = \prod_S B_{b_{S,i}}^\sigma, \quad i = 1, \ldots, t. \tag{C9}$$

Then, for the lhs of the relations, the following is true:

$$B_{b_R} = \prod_{i=1}^{t} B_{b_{R,i}}. \tag{C10}$$

Since all the branes that appear in Eq. (B1) are R branes, the equation can be interpreted in terms of Z_2 chains of $|R|$ cells in the R-shrunk complex. It states that $b_R = b_{R,1} + \cdots + b_{R,t}$. The argument can be reversed; any such dependence between $|R|$ cycles in the R-shrunk complex corresponds to a dependence among relations of the form (B1).

Therefore, counting the number of independent relations of the form (B1) for a given R amounts to counting the number of independent $\mathbf{Z}_2$ chains of closed $|R|$ cycles in the R-shrunk complex. For $|R|=s$, this number is

$$S(D,s) = \sum_{i=0}^{n-s} (-1)^i h_{s+i} + \sum_{i=1}^{n-s} (-1)^i |C_{s+i}|. \tag{C11}$$

This follows by recursion. $S(D,D)=h_0$ and $S(D,s)=h_{D-s} + [|C_{s+1}| - S(D,s+1)]$.

We have to consider all the possible sets R in which r is contained:

$$I_r(D,s) = \sum_{\substack{R \ni r \\ |R|=s}} S(D,s)\big|_{R\text{-shrunk}}. \tag{C12}$$

Then,

$$I(D,s) = I_{\bar{r}}(D,s) + I_r(D,s), \tag{C13}$$

which can be solved and gives

$$I(D,s) = \binom{D}{s-1} \sum_{i=0}^{D-s} (-1)^i h_{s+i} + \sum_{i=0}^{D-s-1} \binom{s+i}{s-1} (-1)^i |C_{s+i+1}|. \tag{C14}$$

Now recall Eq. (22). We can sum up these equations for $r=0,\ldots,s$ with an alternating sign $(-1)^r$. Using the fact that

$$\sum_{i=0}^{a} \binom{b+1}{i} (-1)^i = (-1)^a \binom{b}{a}, \tag{C15}$$

we get

$$\binom{D}{s}\chi = (-1)^s C_0 + \sum_{i=0}^{s-1} \binom{D-i-1}{D-s} (-1)^i |C_{D-i}| + \sum_{i=r+1}^{D} \binom{i-1}{s} (-1)^i |C_i|. \tag{C16}$$

By gathering together Eqs. (C4), (C14), and (C16), we finally obtain Eq. (28).

[1] L. D. Landau, Phys. Z. Sowjetunion **11**, 26 (1937).

[2] V. L. Ginzburg and L. D. Landau, Zh. Eksp. Teor. Fiz. **20**, 1064 (1950).

[3] X.-G. Wen, *Quantum Field Theory of Many-body Systems* (Oxford University Press, 2004).

[4] X.-G. Wen and Q. Niu, Phys. Rev. B **41**, 9377 (1990).

[5] X.-G. Wen, Int. J. Mod. Phys. B **4**, 239 (1990).

[6] X.-G. Wen, Int. J. Mod. Phys. B **6**, 1711 (1992).

[7] A. Kitaev and J. Preskill, Phys. Rev. Lett. **96**, 110404 (2006).

[8] M. Levin and X.-G. Wen, Phys. Rev. Lett. **96**, 110405 (2006).

[9] B. Blok and X.-G. Wen, Phys. Rev. B **42**, 8145 (1990).
[10] N. Read, Phys. Rev. Lett. **65**, 1502 (1990).
[11] J. Froöhlich and T. Kerler, Nucl. Phys. B **354**, 369 (1991).
[12] D. S. Rokhsar and S. A. Kivelson, Phys. Rev. Lett. **61**, 2376 (1988).
[13] N. Read and B. Chakraborty, Phys. Rev. B **40**, 7133 (1989).
[14] R. Moessner and S. L. Sondhi, Phys. Rev. Lett. **86**, 1881 (2001).
[15] E. Ardonne, P. Fendley, and E. Fradkin, Ann. Phys. (N.Y.) **310**, 493 (2004).
[16] V. Kalmeyer and R. B. Laughlin, Phys. Rev. Lett. **59**, 2095 (1987).
[17] X. G. Wen, F. Wilczek, and A. Zee, Phys. Rev. B **39**, 11413 (1989).
[18] N. Read and S. Sachdev, Phys. Rev. Lett. **66**, 1773 (1991).
[19] X.-G. Wen, Phys. Rev. B **44**, 2664 (1991).
[20] T. Senthil and M. P. A. Fisher, Phys. Rev. Lett. **86**, 292 (2001).
[21] X.-G. Wen, Phys. Rev. B **65**, 165113 (2002).
[22] S. Sachdev and K. Park, Ann. Phys. (N.Y.) **298**, 58 (2002).
[23] L. Balents, M. P. A. Fisher, and S. M. Girvin, Phys. Rev. B **65**, 224412 (2002).
[24] F. Verstraete, M. A. Martin-Delgado, and J. I. Cirac, Phys. Rev. Lett. **92**, 087201 (2004).
[25] J. J. Garcia-Ripoll, M. A. Martin-Delgado, and J. I. Cirac, Phys. Rev. Lett. **93**, 250405 (2004).
[26] L.-M. Duan, E. Demler, and M. D. Lukin, Phys. Rev. Lett. **91**, 090402 (2003).
[27] A. Micheli, G. K. Brennen, and P. Zoller, Nat. Phys. **2**, 341 (2006).
[28] J. K. Pachos, quant-ph/0511273 (unpublished).
[29] A. Kitaev, cond-mat/0506438 (to be published).
[30] A. Galindo and M. A. Martin-Delgado, Rev. Mod. Phys. **74**, 347 (2002).
[31] A. Yu. Kitaev, Ann. Phys. (N.Y.) **303**, 2 (2003).
[32] M. H. Freedman, Proc. Natl. Acad. Sci. U.S.A. **95**, 98 (1998).
[33] E. Dennis, A. Kitaev, A. Landahl, and J. Preskill, J. Math. Phys. **43**, 4452 (2002).
[34] S. B. Bravyi and A. Yu. Kitaev, quant-ph/9811052 (to be published).
[35] R. W. Ogburn and J. Preskill, Lect. Notes Comput. Sci. **1509**, 341 (1999).
[36] Michael H. Freedman, Alexei Kitaev, and Zhenghan Wang, Commun. Math. Phys. **227**, 587 (2002).
[37] M. Freedman, M. Larsen, and Z. Wang, Commun. Math. Phys. **227**, 605 (2002).
[38] M. H. Freedman, A. Kitaev, M. J. Larsen, and Z. Wang, Bull., New Ser., Am. Math. Soc. **40**, 31 (2003).
[39] J. Preskill, http://www.theory.caltech.edu/preskill/ph219/topological.ps
[40] H. Bombin and M. A. Martin-Delgado, Phys. Rev. Lett. **97**, 180501 (2006).
[41] H. Bombin and M. A. Martin-Delgado, quant-ph/0605094 (to be published).
[42] H. Bombin and M. A. Martin-Delgado, Phys. Rev. A **73**, 062303 (2006).
[43] W. Thurston, in *Three-dimensional Geometry and Topology*, edited by Silvio Levy, Princeton Mathematical Series Vol. 35 (Princeton University Press, Princeton, NJ, 1997), Vol. 1.
[44] G. Perelman, math.DG/0211159 (unpublished).
[45] G. Perelman, math.DG/0303109 (unpublished).
[46] G. Perelman, math.DG/0307245 (unpublished).
[47] M. A. Levin and X.-G. Wen, Phys. Rev. B **71**, 045110 (2005).
[48] M. Levin and X.-G. Wen, Rev. Mod. Phys. **77**, 871 (2005).
[49] A. Hamma, P. Zanardi, and X.-G. Wen, Phys. Rev. B **72**, 035307 (2005).
[50] C. Wang, J. Harrington, and J. Preskill, Ann. Phys. (N.Y.) **303**, 31 (2003).
[51] K. Takeda and H. Nishimori, Nucl. Phys. B **686**, 377 (2004).
[52] F. Wilczek, Phys. Rev. Lett. **49**, 957 (1982).
[53] J. M. Leinaas and J. Myrheim, Nuovo Cimento Soc. Ital. Fis., B **37**, 1 (1977).
[54] D. Gottesman, Phys. Rev. A **54**, 1862 (1996).